

Band Structure and Electron Transport of GaAs

H. EHRENREICH

General Electric Research Laboratory, Schenectady, New York

(Received August 8, 1960)

Existing experimental data on GaAs are reviewed and analyzed to yield the band structure in the vicinity of the band edges as well as the parameters characterizing the bands summarized in Fig. 1 of this paper. On the basis of presently existing experimental evidence, chiefly the behavior of the optical band gap in Ga(As,P) alloys and the deduced pressure shift and density of states effective mass, it is thought likely that the subsidiary conduction band minima lie along $[100]$ directions. Analytical expressions including nonparabolic effects are given for the energy and density of states of the $[000]$ conduction band and used to obtain a better value of the effective mass from optical reflectivity data. The experimentally observed structure in the Hall effect in n -type material at elevated temperatures is shown to result from excitation of carriers into the subsidiary conduction band. Changes of resistivity with

pressure are explained on the basis of an increase of the $[000]$ effective mass at low pressures and the transfer of carriers to the subsidiary minima at higher pressures. The scattering mechanisms, which are important in connection with transport phenomena, are shown to be polar lattice scattering and charged impurity scattering in the highest mobility samples. The transport calculations leading to the mobility and thermoelectric power as a function of temperature and impurity concentrations are performed using variational techniques, and shown to agree well with experiment. The apparently low mobility in the subsidiary minima is attributed at least in part to the large effective mass and relatively small anisotropy ratio. An estimate shows scattering between the two conduction bands probably to be unimportant.

I. INTRODUCTION

A FAIR amount of experimental information concerning GaAs has been accumulated over the past few years. This information, together with evidence resulting from the study of closely related semiconductors having the diamond and zinc-blende structures, permits the deduction of information concerning the band structure in a region extending a few tenths of a volt from both conduction and valence band edges. In this paper we shall present evidence that the band structure and results shown in Fig. 1 are the most reasonable on the basis of present experimental data and show that they lead to a consistent account of the properties of GaAs. Because the available data are more satisfactory and complete, we shall emphasize the properties of n -type material.

Partial interpretations in terms of a model for the band structure proposed by Callaway,¹ to be described below, have already been given in some of the papers setting forth the experimental results to be dealt with here. In the following two sections, concerned with the band structure, these will be reviewed. In Sec. II we shall show that the band structure at the band edges is very similar to that of InSb,² and on this basis shall present expressions estimating the nonparabolicity of the conduction band which permit a reliable determination from the available experimental data^{3,4} of the effective conduction band mass at the minimum. We shall also obtain some estimates of the valence band masses.⁵ Section III is concerned with the excited conduction bands. We shall show that the model of Fig. 1, with the subsidiary conduction band minima located along $[100]$ directions, is able to account for the

resistivity as a function of pressure,⁶ the Hall effect at elevated temperatures,⁷ and the behavior of the band gap in Ga(As,P) alloys.⁸ In Sec. IV we shall examine the scattering mechanisms determining the transport properties of GaAs. Polar scattering will be shown to dominate the mobility above room temperature, as in InSb,^{9,10} InP, and InAs,¹¹ and a combination of polar and charged impurity scattering will be seen to yield agreement with the experimental mobility in the purest samples as a function of both temperature and impurity concentration. The calculated thermoelectric power will also be shown to agree well with experimental data.

II. CONDUCTION BAND EDGE AND VALENCE BANDS

The first theoretical comments concerning the band structure of GaAs, made by Herman,¹² stressed the similarity to the germanium band structure. Callaway,¹ working along lines suggested by Herman, obtained results for GaAs by a perturbation procedure. He concluded that it was likely that the conduction band minimum occurred at the center of the Brillouin zone, and pointed to thermoelectric power measurements,¹³ which suggested that the conduction band mass might be much smaller than in germanium, as supporting evidence. Experimental work on optical reflectivity,¹⁴ the magnetoresistance experiments of Glicksman,¹⁵ and the

⁶ W. Howard and W. Paul (to be published).

⁷ L. W. Aukerman and R. K. Willardson, *J. Appl. Phys.* **31**, 939 (1960).

⁸ H. Welker and H. Weiss, *Solid State Physics*, edited by F. Seitz and D. Turnbull (Academic Press, New York, 1956), Vol. 3.

⁹ H. Ehrenreich, *J. Phys. Chem. Solids* **2**, 131 (1957).

¹⁰ H. Ehrenreich, *J. Phys. Chem. Solids* **9**, 129 (1959).

¹¹ H. Ehrenreich, *J. Phys. Chem. Solids* **12**, 97 (1959).

¹² F. Herman, *J. Electronics* **1**, 103 (1955).

¹³ R. Barrie, F. A. Cunnell, J. T. Edmond, and I. M. Ross, *Physica* **20**, 1087 (1954).

¹⁴ L. C. Barcus, A. Perlmutter, and J. Callaway, *Phys. Rev.* **111**, 167 (1958); **115**, 1778(E) (1959).

¹⁵ M. Glicksman, *J. Phys. Chem. Solids* **8**, 511 (1959).

¹ J. Callaway, *J. Electronics* **2**, 330 (1957).

² E. O. Kane, *J. Phys. Chem. Solids* **1**, 249 (1957).

³ W. G. Spitzer and J. M. Whelan, *Phys. Rev.* **114**, 59 (1959).

⁴ T. S. Moss and A. K. Walton, *Proc. Phys. Soc. (London)* **74**, 131 (1959).

⁵ R. Braunstein, *J. Phys. Chem. Solids* **8**, 280 (1959).

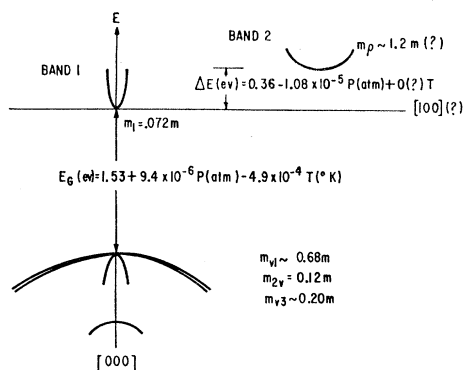


FIG. 1. Schematic diagram showing band structure of GaAs in the vicinity of the conduction and valence band edges. Parameters and numerical results are deduced or discussed in Secs. 2 and 3 of text.

elastoresistance studies of Sagar,¹⁶ which showed the surfaces of constant energy to be spherical, gave further support to this model. Reliable values of the effective mass were obtained from the optical reflectivity experiments of Spitzer and Whelan,³ which yielded an electron mass $m_1 = (0.078 \pm 0.004)m$, and the Faraday rotation experiments of Moss and Walton⁴ which gave $m_1 = 0.072 (+0.008, -0.005)m$.

Evidence that the valence bands are similar to those of germanium was furnished by the free hole absorption measurements of Braunstein.⁵ These experiments yielded a value of the spin-orbit splitting of $\Delta = 0.33$ eV as well as ratios of the effective masses in the heavy mass, light mass, and split-off bands.

From the preceding information and the fact that the shape of the fundamental optical absorption edge^{8,3} appears to be consistent with direct transitions, it may be concluded that the band structure of GaAs in the immediate vicinity of the edge is very similar to that of InSb. Thus Kane's theory² for the latter material can be immediately adapted and used to untangle experimental valence band mass ratios and to estimate the deviation from parabolicity of the conduction band. A simple expression for the dependence of the conduction band energy $E(k)$ on wave number is obtained from Kane's more general expression with the aid of the approximation, valid in GaAs, that the band gap E_G is much larger than the spin-orbit splitting energy Δ :

$$E(k) = (\hbar^2 k^2 / 2m) + (E_G / 2) \times [(1 + 4E_P \hbar^2 k^2 / 2mE_G)^{1/2} - 1]. \quad (1)$$

From the known effective mass near the bottom of the conduction band the value $E_P = 2mP^2/\hbar^2 = 20$ eV may be deduced. Here P is the momentum matrix element connecting the conduction, light mass, and split-off valence bands. Inserting this value into the third of Eqs. (12) in reference 2 we obtain $m_{v2} = 0.12m$ and with the help of the experimentally determined mass ratios

the values $m_{v1} = 0.68m$ and $m_{v3} = 0.20m$. These same equations also lead directly to the mass ratio m_3/m_2 . We find $m_3/m_2 = 2.5$ as compared to the value of 1.7 quoted by Braunstein. In the absence of a detailed theory to fit the experimental data, this must be regarded as satisfactory agreement, and perhaps indicative of the accuracy of the valence band masses determined in this way.

It is of interest that the energy E_P , as deduced from experimental information, entering Eq. (1) is practically a constant for InSb, InAs, GaSb, InP, and GaAs. This fact together with the information that the transport properties are entirely consistent with a conduction band at [000] further substantiates the belief that the band structure of GaAs in the immediate vicinity of the band gap is similar to that of InSb. Nonparabolic effects in the conduction band of GaAs are relatively unimportant, in contrast to InSb,^{2,9} and may be approximated by expanding Eq. (1) to terms in k^4 . However, it is undoubtedly these effects that are responsible for the small discrepancy in the effective masses determined by Spitzer and Whelan³ and Moss and Walton.⁴ The value $m_1 = 0.072m$ was obtained on lightly doped samples containing fewer than 5×10^{16} cm⁻³ carriers, whereas the larger value corresponded to samples containing almost ten times as many carriers.

In an earlier paper¹⁰ we showed how to modify the type of analysis used by Spitzer and Whelan³ to apply to nonparabolic bands. With this theory the experimentally determined effective mass m_{exp} appearing in the formula for the susceptibility³ $\chi_c = -ne^2/m_{\text{exp}}\omega^2$ is related to the true [000] conduction band effective mass m_1 in GaAs by the equation

$$m_{\text{exp}}^{-1} = m_1^{-1} [1 - (10/3)(1 - m_1/m)^2 (KT/E_G) \times (2\pi^2 n)^{-1} (2KTm_1/\hbar^2)^{3/2} F_{3/2}(z)]. \quad (2)$$

Here n is the carrier concentration, z the Fermi energy divided by KT , $F_{3/2}$ a Fermi-Dirac integral,¹⁷ and ω the frequency of the light. In deriving Eq. (2) we have used Eq. (1) and the relationship

$$n = (2\pi^2)^{-1} (2m_1KT/\hbar^2)^{3/2} \times [F_{3/2}(z) + (5/2)(KT/E_G)(1 - m_1/m)^2 F_{3/2}(z)], \quad (3)$$

which determines the Fermi level for a given extrinsic electron concentration n in the nonparabolic conduction band of GaAs if the donor ionization energy is taken to be zero. Applying Eq. (2) to the results of reference 3 we find that the effective mass m_1 at the bottom of the band should be $0.072m$, $0.072m$, and $0.075m$, for samples 3, 4, and 6, respectively, rather than the values $0.078m$, $0.079m$, $0.089m$ for these samples deduced directly from experiment. The best determination of the effective mass at the edge of the [000] minimum from these experiments therefore appears to be $m_1 = 0.072m$.

¹⁶ A. Sagar, Phys. Rev. **112**, 1533 (1958).

¹⁷ A. H. Wilson, *The Theory of Metals* (Cambridge University Press, New York, 1953), 2nd ed., p. 331.

III. EXCITED CONDUCTION BANDS

Callaway's calculations predicted the existence of a conduction band edge in the [111] direction a few tenths of a volt above the [000] minimum. The position of the [100] minimum was not quantitatively estimated in this work, but it too would be expected to be nearby as in germanium. Gray and Ehrenreich¹⁸ advanced an explanation for the increase in the Hall coefficient in *n*-type material occurring just before the onset of intrinsic conduction^{19,20} on the basis of Callaway's model. The effect was attributed to two-band conduction that set in at temperatures above 500°K when electrons could be evaporated into the higher conduction band. An energy separation of 0.2 to 0.4 eV between the minima was found to be consistent with the experimental data. This view was confirmed by the electron free carrier absorption measurements of Spitzer and Whelan⁹ which exhibited a threshold for an additional absorption process at about 0.25 eV. This threshold was associated with transitions to the [111] minima.

The optical measurements of band gap as a function of pressure by Edwards *et al.*²¹ showed an initial blue shift followed by a red shift above 60 000 atmospheres. This was interpreted as evidence for the existence of a [100] minimum about 0.5 eV above the [000] minimum at atmospheric pressure.

In this section a detailed analysis of data of Aukerman and Willardson⁷ on the Hall coefficient at high temperatures will be shown to lead to a set of parameters which can be used to explain the effect of pressure on the resistivity as observed by Howard and Paul,⁶ if it is assumed that the subsidiary minima have approximately the same variation with pressure as the [100] minima of silicon, and that the value $\partial E_{000}/\partial P = 9.4 \times 10^{-6}$ eV/atm for the pressure change of the [000] minimum quoted in reference 21 is correct. Further, data on the variation of band gap with composition in Ga(As,P) alloys will be used to show that the energetic position of the subsidiary minima is consistent with their location along [100] directions. The section will close with a discussion of other optical properties relevant to this problem.

A. Hall Effect

The Hall coefficient for multiband conduction may be written in the form

$$R_H = -(ec)^{-1} [\sum_i G_i n_i \mu_i^2] / [\sum_i n_i \mu_i]^2, \quad (4)$$

where n_i and μ_i are, respectively, the carrier concentration and mobility for band i , as labelled in Fig. 1, and G_i is a factor depending on the scattering mechanisms,

the average inertial masses associated with the mobility and Hall coefficient²² which are different in the case of ellipsoidal energy surfaces, and the sign of the charge carrier. Equation (4) is valid provided that interband scattering among the bands i is sufficiently weak. It can be shown that for polar scattering G_1 and G_2 may be taken as unity within 10% and 20%, respectively. The valence bands enter the present calculations only insensitively at the onset of the intrinsic range and we shall take $G_i = 1$ for them as well.

The analysis of Gray and Ehrenreich¹⁸ as well as that of Aukerman and Willardson⁷ was based on Eq. (4) in the limit of two electron bands contributing to the conduction. Aukerman and Willardson made the interesting observation that a plot of $\log[(R_H - R_H^{(0)})/R_H^{(0)}] = \log(\Delta R/R)$, the relative increase of the Hall coefficient R_H due to multiband conduction (as compared to its value $R_H^{(0)}$ when only one band is involved but all donors are fully ionized) vs T^{-1} permits a determination of ΔE , the energy difference between the two bands at zero temperature. Their data were fitted on the assumption that the mobility ratio $b = \mu_1/\mu_2 = 10$, whereas we shall see from the pressure experiments that the ratio may actually be considerably larger, and that a more consistent assumption may be to take $b = \infty$. In that case Eq. (4) becomes

$$R_H = [n_1(T)ec]^{-1}, \quad (5)$$

where $n_1(T)$ is the number of carriers present in band 1 at temperature T . Since below the onset of intrinsic conduction the total number of carriers distributed between bands 1 and 2 at temperature T must be equal to the number in band 1 for the conditions under which R_H^0 is measured, we have:

$$\begin{aligned} \Delta R(T)/R &= (R_H - R_H^0)/R_H^0 = b_p \exp[-\Delta E(T)/KT] \\ &= b_p \exp(-K^{-1} \partial \Delta E / \partial T) \exp[-\Delta E(0)/KT] \\ &= b_p^* \exp[-\Delta E(0)/KT], \quad (6) \end{aligned}$$

where $b_p = (m_p/m_1)^3$ and m_p is the density of states mass in band 2. Equation (6) supposes Boltzmann statistics to be applicable, which is true for the elevated temperature range under consideration here. The last members of this equation are obtained by assuming that the gap varies linearly with temperature.

A re-evaluation of the Battelle data on the basis of Eq. (5) leads to $\Delta E(0) = 0.36$ eV which is somewhat smaller than their value of 0.38 eV, but still lies within the quoted error. The analysis also yields a value of $b_p^* = 70(+40, -20)$. If it be supposed that $\partial \Delta E / \partial T$ is very small, as it might well be since many of the band edges studied in the group 4 and 3-5 semiconductors move at essentially the same rate with temperature, then we may deduce a rough value for the density of states mass from the Hall data. We find $m_p = 1.2(+0.5, -0.3)$ which is reasonably close to the value $m_p = 1.1$ found for the [100] minimum in silicon.

¹⁸ P. V. Gray and H. Ehrenreich, *Bull. Am. Phys. Soc.* **3**, 255 (1958).

¹⁹ O. G. Folberth and H. Weiss, *Z. Naturforsch.* **10a**, 615 (1955).

²⁰ J. T. Edmond, R. F. Broom, and F. A. Cunnell, *Rugby Semiconductor Conference* (The Physical Society, London, 1956).

²¹ A. L. Edwards, T. E. Slykhouse, and H. G. Drickamer, *J. Phys. Chem. Solids* **11**, 140 (1959).

²² C. Herring, *Bell System Tech. J.* **34**, 237 (1955).

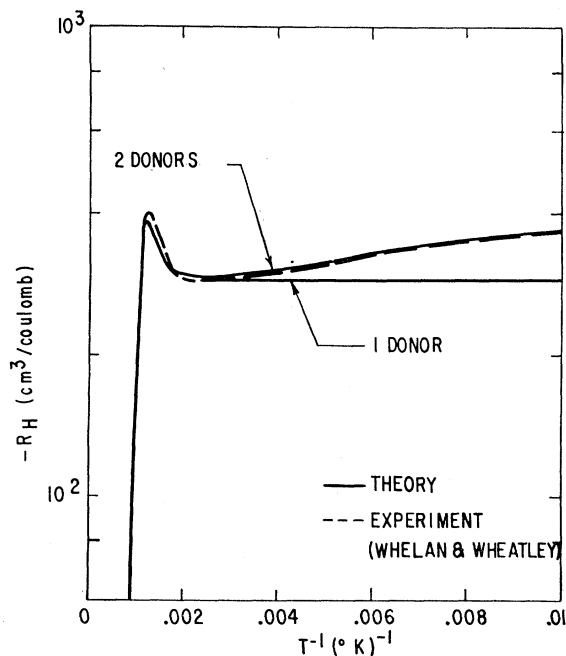


FIG. 2. Hall coefficient vs reciprocal temperature. Theoretical curves assume single donor with zero activation energy and two donors with zero and 0.04-eV activation energies in 10:1 ratio. Total carrier concentration is $2.2 \times 10^{16} \text{ cm}^{-3}$.

However, most of the present calculations require knowledge of only b_p^* since the Fermi level at elevated temperatures when Boltzmann statistics are valid depends on b_p^* rather than b_p , and as will be seen, it is also b_p^* that enters the theory for the pressure experiments.

A complete Hall curve extending from low temperatures into the intrinsic range has been calculated and is shown in Fig. 2 in comparison to measurements of an *n*-type sample by Whelan and Wheatley.²³ The formula for the Hall coefficient given by Eq. (4) has been generalized to include the influence of the valence bands in the intrinsic range. Polar scattering is assumed to dominate in each band. Scattering between the valence bands has been treated roughly in the relaxation time approximation assuming, in analogy with treatments of *p*-type germanium,²⁴ that the light holes scatter into the heavy-mass band, and the heavy holes remain in that band by density of states arguments. In order to fit the low-temperature portion of the curve, we have used the assumption suggested in reference 23, that there are actually two types of donors present, the first having zero activation energy and the second with activation energy 0.04 eV. The concentrations are supposed to be 2.0×10^{16} and 0.2×10^{16} , respectively. To show that all this does not affect the high-temperature behavior seriously, we have also included a curve calculated on the

²³ J. M. Whelan and G. H. Wheatley, *J. Phys. Chem. Solids* **6**, 169 (1958).

²⁴ H. Brooks, *Advances in Electronics*, edited by L. Marton (Academic Press, New York, 1956), Vol. 7.

assumption that all donors have zero activation energy. Both the shape and the maximum of the Hall coefficient above 500°K are seen to be represented quite well by the present theory. Since the valence bands appear in a relatively insensitive way in the present calculations, our treatment of the scattering in these bands should not be considered as proof that polar scattering is the only operative mechanism.²⁵

B. Pressure Experiments

The increase of resistance with pressure in *n*-type GaAs may be expected to be brought about at low pressures primarily by the increase in effective mass of the [000] minimum due to the widening band gap, and at higher pressures by the decrease of ΔE and the resultant transfer of electrons from the [000] to the heavier subsidiary minima. The data of Howard and Paul⁶ for an extended pressure range up to about 30 000 atmospheres and that of Sagar²⁶ over a more limited range confirm this expectation. The analysis to be presented here is based on the following assumptions: (1) The experimental data fall in the extrinsic range, (2) Boltzmann statistics are applicable, (3) polar scattering is dominant at room temperature, (4) the mobility in the [100] valleys is very much smaller than that in the [000] minima, and (5) scattering between the [000] and [100] valleys may be neglected. Assumptions (1) and (2) are satisfied at room temperature and for the carrier concentrations ($< 10^{17} \text{ cm}^{-3}$) present in the measured samples. Assumption (3) may be valid for Sagar's samples for which $\mu = 4000 \text{ cm}^2/\text{volt-sec}$ at 77°K. It is rather questionable for the samples measured by Howard and Paul, one of which (*LLA*) had a mobility of only $1800 \text{ cm}^2/\text{volt-sec}$ at room temperature. However, the results will be seen to be relatively insensitive to the scattering mechanism except at low pressures. The validity of assumption (4) is confirmed by the subsequent analysis and that of assumption (5) will be discussed in Sec. IV.

By assumption (1) we may express the carrier concentrations $n_1(P)$ and $n_2(P)$ in bands 1 and 2 at pressure P and room temperature in terms of the total carrier concentration $n_1(0)$ in band 1 at zero pressure, by the equation $n_1(P) + n_2(P) = n_1(0)$. Using the standard expressions for multiband conduction, whose validity de-

²⁵ A preliminary analysis of some very recent data from Battelle [Report to the Compound Semiconductor Research Group, Battelle Memorial Institute, 1960 (unpublished)] on the mobility in *p*-type GaAs as a function of temperature using the masses shown in Fig. 1, assuming the mobility in band ν_2 to be determined by polar scattering, and treating interband scattering along the lines suggested here, shows fairly good agreement with experiment and suggests that this mechanism may be predominant also in the valence bands. This is a little surprising since nonpolar optical mode scattering and deformation potential scattering should contribute here because the electron wave function has *p* symmetry and the effective masses are reasonably large. If these mechanisms are indeed important, it may be that the value of m_{ν_1} is somewhat smaller than is indicated on Fig. 1.

²⁶ A. Sagar, Westinghouse Research Report 6-40602-3-R1, May, 1959 (unpublished).

depends on assumption (5), we find the following expression for the resistivity ratio at pressure P to that at atmospheric pressure:

$$\rho(P)/\rho(0) = [\mu_1(0)/\mu_1(P)] \{1 - [n_2(P)/n_1(P)] \times [1 - \mu_2(P)/\mu_1(P)]\}^{-1}. \quad (7)$$

It is seen that when $\mu_2(P) \ll \mu_1(P)$, Eq. (7) becomes

$$\rho(P)/\rho(0) = [\mu_1(0)/\mu_1(P)] [1 - n_2(P)/n_1(0)]^{-1}. \quad (8)$$

Thus, if the gap between bands 1 and 2 diminishes with pressure, and density of states in band 2 is much larger than that in band 1 most of the carriers are transferred into this band. Thus $\rho(P)/\rho(0)$ increases without limit as $n_2(P)/n_1(0) \rightarrow 1$. Such behavior is the most remarkable feature of the data of Howard and Paul shown in Fig. 4. The resistivity is seen to increase rapidly with pressure and shows no tendency to saturate. This indicates that $\mu_1 \gg \mu_2$. Ultimately, however, one would expect $\rho(P)/\rho(0)$ to saturate at a value $\mu_1(0)/\mu_2(P)$. Extension of the data to higher pressures would permit a determination of this ratio.

It is convenient to rewrite Eq. (7) in a form which will permit a graphical deduction of $\partial\Delta E/\partial P$ as well as direct comparison with the information obtained from the Hall data discussed in the preceding subsection. Following assumptions (2) and (3) we may write:

$$n_2(P)/n_1(P) = [m_p/m_1(P)]^{3/2} \exp[-\Delta E(P)/KT], \quad (9)$$

and

$$\mu_1(P)/\mu_1(0) = [m_1(0)/m_1(P)]^{3/2}. \quad (10)$$

We thus find

$$\rho(P)/\rho(0) = [m_1(P)/m_1(0)]^{3/2} + b_p \exp[-\Delta E(P)/KT]. \quad (11)$$

Writing

$$\Delta E(P) = \Delta E(0) + (\partial\Delta E/\partial T)_P T + (\partial\Delta E/\partial P)_T P, \quad (12)$$

where $\Delta E(0)$ is the gap between bands 1 and 2 at atmospheric pressure and 0°K , and using Eq. (6), we obtain

$$\rho(P)/\rho(0) = [m_1(P)/m_1(0)]^{3/2} + [\Delta R(T)/R] \times \exp[-(\partial\Delta E/\partial P)(P/KT)]. \quad (13)$$

The behavior of the resistivity as a function of pressure is thus expressible as a sum of two terms: the first reflecting the increase in effective mass of band 1 with pressure and the second the decreasing separation of bands 1 and 2 and the consequent transfer of carriers from the high- to the low-mobility band. The coefficient of the second term is just the change in Hall coefficient with temperature described by Eq. (6), but extrapolated back to room temperature. Thus a semilogarithmic plot of $\rho(P)/\rho(0) - [m_1(P)/m_1(0)]^{3/2}$ vs P leads to a determination of $\partial\Delta E/\partial P$ from the slope²⁷ and also of $\Delta R(300)/R$

²⁷ The idea of determining the relative rate of motion of two conduction bands with pressure from a similar type of semilogarithmic

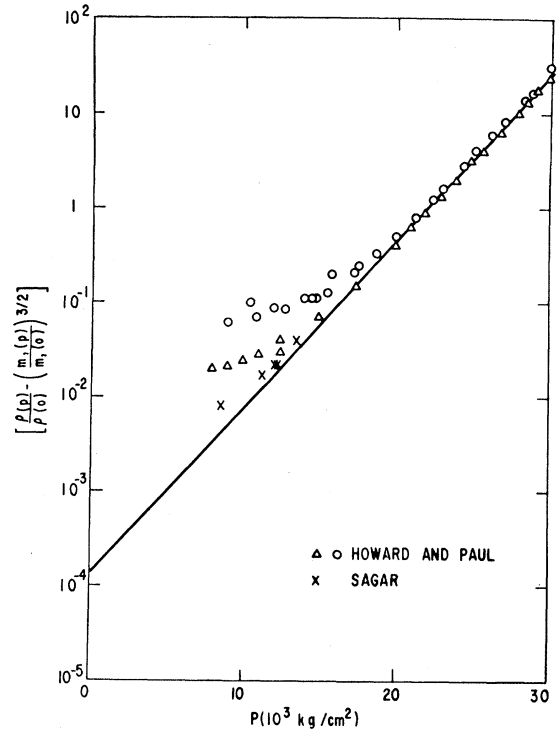


Fig. 3. Plot used to determine $\partial\Delta E/\partial P$ and $\Delta R(300^\circ\text{K})/R$.

at 300°K from the intercept. This provides a check of the mutual consistency of the pressure and Hall data. The ratio $m_1(P)/m_1(0)$ can be determined in the manner used in reference 9. Using Kane's theory² and assuming that E_p [see Eq. (1)] and the spin-orbit splitting Δ are essentially independent of pressure, we find:

$$\begin{aligned} m_1(P)/m_1(0) &= [E_G(P)/E_G(0)] \{1 + \frac{1}{2}E_G(0)[E_G(0) + \Delta]^{-1}\} / \\ &\quad \{1 + \frac{1}{2}E_G(P)[E_G(P) + \Delta]^{-1}\}. \end{aligned} \quad (14)$$

If polar scattering is not the dominant mechanism then the exponent $\frac{3}{2}$ which appears in Eq. (10) is altered. From Eq. (8) it follows that $\rho(P)/\rho(0)$ is therefore multiplied by a factor $[m_1(P)/m_1(0)]^{n-\frac{3}{2}}$, when it is valid to write the dependence on the effective mass as a power law, where n is the exponent that replaces $\frac{3}{2}$ in Eq. (10). Since the variation of $m_1(P)$ is rather small, the nature of the scattering mechanism will only affect the results significantly in the low-pressure range, provided b is large.

The plot in question is shown in Fig. 3. The data of Howard and Paul⁶ at high pressures and that of Sagar²⁶ at lower pressures are seen to fall on a reasonable straight line. There are significant deviations at pressures below about 18 000 atmospheres for the samples

rithmic plot was applied earlier to germanium by H. Brooks and W. Paul [Bull. Am. Phys. Soc. 1, 48 (1956)] and also by M. I. Nathan [Harvard University Technical Report No. HP-1, February, 1958 (unpublished)]. I am indebted to W. Paul for pointing this out.

measured by Howard and Paul, which may be due, at least in part, to the fact that polar scattering is not dominant at room temperature. On the other hand, Sagar's data which appears to originate from a higher mobility sample does not deviate as much from the same straight line.

The values obtained from the slope and the intercept are: $\partial\Delta E/\partial P = -(1.08 \pm 0.04) \times 10^{-5}$ ev/atm and $\Delta R(300)/R = b_p^* \exp[-\Delta E(0)/300^\circ\text{K}] = (1.4 \pm 0.4) \times 10^{-4}$. The value of $\Delta R/R$ should be contrasted with the number $\Delta R(300)/R = 8.6 \times 10^{-5}$ obtained by inserting the values for b^* and $\Delta E(0)$ obtained from the Hall data. Because of the error of ± 0.02 ev assigned to $\Delta E(0)$, and that involved in the determination of $\Delta R(300)/R$, the 50% difference between the two determinations of $\Delta R/R$ lies within the experimental uncertainty.

Using the preceding value for $\partial\Delta E/\partial P$ and the result $\partial E_{000}/\partial P = 9.4 \times 10^{-6}$ ev/atm quoted by Edwards *et al.*,²¹ we find the shift with pressure of the subsidiary minimum to be -1.4×10^{-6} ev/atm. This value is reasonably close to that observed for the [100] minima in silicon, and would thus support the view that the subsidiary minima in GaAs lie along these directions as well. Implicit in this statement is the empirical hypothesis, that a given type of conduction band valley in any of the group 4 and 3-5 semiconductors, behaves in the same way under pressure.^{28,29}

The behavior of the calculated $\rho(P)/\rho(0)$ as a function of pressure is shown in Fig. 4 to indicate the extent to which Eq. (13) fits the actual data of Howard and Paul.⁶ The solid line is obtained when $\Delta R/R$ and $\Delta E(0)$ resulting from the analysis of Fig. 3 are used and the dashed line is obtained when the value of $\Delta R/R$ is deduced from the Hall data. The inset represents an expansion of the resistivity scale for small pressures, and shows both the data of Howard and Paul and of Sagar.

A rough estimate of the lower bound of the mobility ratio $b = \mu_1/\mu_2$ made from the present calculation, indicate that it is very unlikely that b is smaller than 50.

C. Optical Experiments

There are several experiments involving optical absorption that also provide information concerning the subsidiary conduction band minima. These are (1) free carrier absorption measurements³ in the region between 1 and 25 μ , (2) measurements on the fundamental optical absorption in Ga(As,P) alloys,³⁰ and (3) the observations of fundamental optical absorption at ele-

vated pressures.²¹ We shall discuss the interpretation of these experiments briefly.

Spitzer and Whelan³ found an absorption edge at about 0.25 ev in *n*-type GaAs, which they interpreted in terms of Callaway's model¹ as arising from transitions between the [000] and [111] minima. This room temperature value disagrees by more than 0.1 ev with the result for the gap at 0°K determined from the Hall data. The most likely source for this discrepancy is the fact that some of the samples used in the experiments were heavily doped, so that, at least at low temperatures, the measured threshold would actually correspond to the energy interval between the Fermi level and the subsidiary minimum plus the energy of the phonon involved in the transition. For the most heavily doped samples used in these experiments, the Fermi level at room temperature lies about 0.15 ev above the band edge. This is

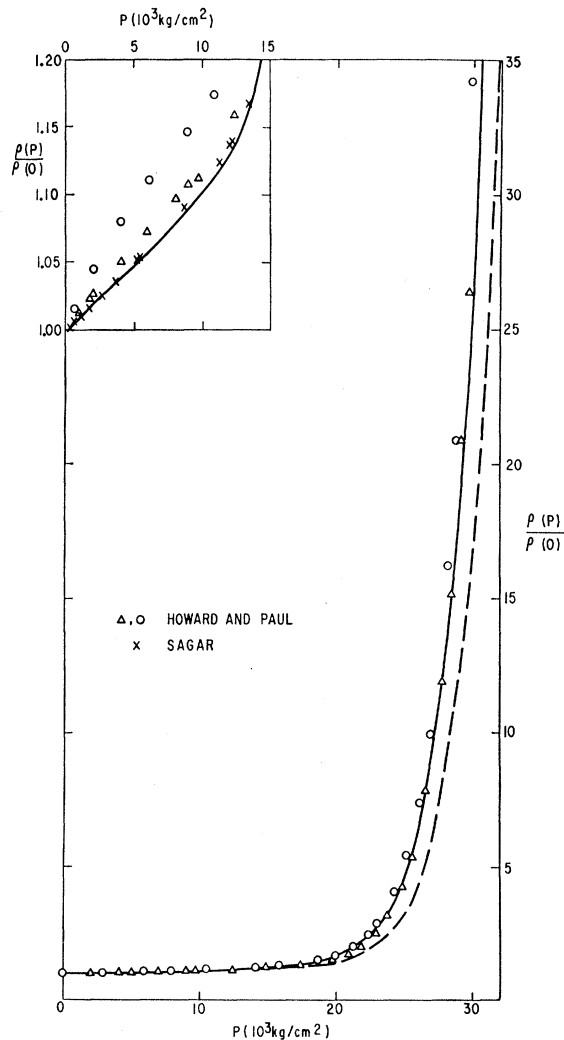


FIG. 4. Normalized resistivity vs pressure. Solid and dashed curves calculated using parameters deduced from Fig. 3 and Hall data, respectively. Inset shows vertically expanded plot at low pressures.

²⁸ W. Paul, J. Phys. Chem. Solids 8, 196 (1959).

²⁹ Unpublished preliminary measurements by W. Paul and D. Warschauer lead to a value for $\partial E_{000}/\partial P$ which is about 25% higher than that quoted by Edwards *et al.*²¹ If this value is substantiated by further measurements currently in progress, the rate of change of the subsidiary minima with pressure would turn out to be slightly positive, but not nearly as large as the value $+5 \times 10^{-6}$ ev/atm observed for the [111] minima in germanium.²⁸

³⁰ O. G. Folberth, quoted by Welker and Weiss, reference 8, p. 53.

more than enough to reconcile the observed ΔE with that observed from the Hall measurements. For the more lightly doped samples the data are not inconsistent with a shift of the threshold to somewhat higher energies.

We have not made a detailed calculation to fit the data, since the shapes of the experimental curves (see reference 3, Fig. 2) are the result of a subtraction procedure that may be inaccurate in the region near the threshold of the process which is of greatest theoretical interest. Further, it is difficult to arrive at a quantitative theory since neither the electron-phonon mechanism that scatters an electron between the two sets of minima, nor the phonon energies involved are known. Since the strength of the polar interaction falls off rapidly as the phonon wavelength becomes smaller, it is unlikely to dominate in weakly polar crystals, for phonons that span a large fraction of the Brillouin zone.

The possibility, mentioned also by Aukerman and Willardson,⁷ that the discrepancy arises from a temperature dependence of $\Delta E(T)$, appears unlikely, since this would lead to a value of $\partial\Delta E/\partial T = -3.7 \times 10^{-4}$ eV/°K, and with the help of the known value of $\partial E_G/\partial T = -4.9 \times 10^{-4}$ eV/°K³¹ to the result -8.6×10^{-4} eV/°K for the temperature shift of the subsidiary minima. This is about twice as large as typical values observed in related materials. Further, we shall see that it is possible to estimate $\Delta E(300)$ to be about 0.40 eV from the data on Ga(As,P) alloys. This implies a very small or zero temperature shift which seems to be more reasonable.

We now turn to a discussion of the Ga(As,P) data. In their review article Welker and Weiss⁸ show a curve, derived from fundamental optical absorption data by Folberth, of the band gap as a function of composition for these alloys ranging from 0 to 100% As. This curve is shown by the solid line in Fig. 5. From the pressure experiments of Edwards *et al.*,²¹ the lowest conduction band minimum in GaP is believed to lie along [100] directions,³² and as pointed out already, the lowest conduction band minimum in GaAs is located at [000]. Hence, the break in the curve in Fig. 5 near the 50% composition may be attributed to a switch-over between these two sets of minima, if it is assumed that the valence band structure remains unchanged over the entire range of compositions. Since the curve drawn through the experimental points appears to consist of two straight line segments, each extending over approximately half the range of compositions, it may be legitimate to extrapolate them back, as is done by the dashed lines shown in Fig. 4 to the GaAs and GaP sides, respectively. The energies determined in this way should provide an estimate of the energetic position of these bands with respect to the lowest conduction band minima in the two materials. On the GaAs side the gap

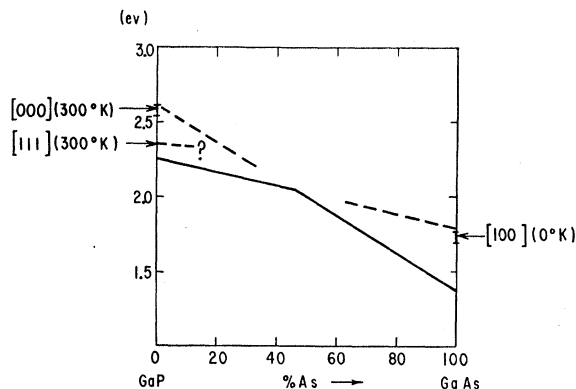


FIG. 5. Band gap vs composition in Ga(As,P) alloys. Solid curve: data of Folberth. Dashed curve: extrapolation of straight line segments to GaAs and GaP sides. "I"-shaped points: energetic positions of [000] and [100] minima on GaP and GaAs sides, respectively, as deduced from independent evidence.

between the [000] and [100] minima is determined to be 0.40 eV, which is to be compared to the value 0.36 ± 0.03 eV obtained from the Hall data. On the GaP side the separation between these same sets of minima, but with the [100] energetically lower, is 0.35 eV. This value is to be compared with optical data by Spitzer *et al.*³³ on both fundamental and free carrier absorption in *n*-type GaP which yield separations of 0.35 eV and 0.31 eV, respectively. These experiments therefore indicate that the [100] minima are located energetically in the region required by the Hall and pressure data.

The experiments of Edwards *et al.*²¹ on GaAs at high pressures also indicate that the [100] minima lie energetically close to the band edge. The results show an initial increase of the optical band gap with pressure. At 60 000 atm the gap becomes a maximum and decreases subsequently with an approximate slope of -8.7×10^{-6} eV/atm. This reversal is associated with the [100] minima. It should be noted, however, that in this high-pressure range there are certain irreversible effects, which are attributed to disordering transformations.

If the subsidiary conduction band edge is associated with [100] minima, as is suggested by the evidence already discussed, then the pressure variation of the gap between the [000] and [100] minima deduced from the data of Howard and Paul,⁶ together with their separation at atmospheric pressure of about 0.36 eV, lead to the conclusion that the [100] minima become lowest at 33 000 atm, rather than at 60 000 atm.

One might try to reconcile the contradiction with the results of reference 21 by postulating the conduction band structure discussed previously^{18,34} in which the [111] minima constitute the subsidiary edge involved in the pressure and Hall data just discussed, and the [100] minima lie energetically higher. This might, on the

³¹ See reference 8, p. 51.

³² Unfortunately, to the time of writing this conclusion has not yet been independently confirmed from either magnetoresistance or elasto-resistance measurements.

³³ W. G. Spitzer, M. Gershenzon, C. J. Frosch, and D. F. Gibbs, *J. Phys. Chem. Solids* **11**, 339 (1959).

³⁴ H. Ehrenreich and D. J. Olechna, *Bull. Am. Phys. Soc.* **5**, 151 (1960).

surface, appear to be reasonable, particularly if the larger pressure shift of the [000] minimum tentatively quoted by Paul and Warschauer³³ were confirmed in their further experiments. One would then assign a value $\partial E_{111}/\partial P \lesssim +2 \times 10^{-6}$ ev/atm to the pressure coefficient of the [111] minimum. By assuming the [100] minima to lie about 0.6 ev above the edge at atmospheric pressure, and to shift with pressure like those of silicon, it would be possible to obtain the reversal at 60 000 atm observed by Edwards *et al.* However, even in this case a drastic reduction of slope at 33 000 atm of almost a factor of six is required. Such a change is not evident in the data of reference 21. Further, the shift assigned to the [111] minima would be more than a factor of two smaller than the coefficient for the corresponding minima in germanium, which is somewhat unreasonable.

Finally, it should be noted that the reversal observed in these experiments represents a change from a direct to an indirect optical transition. It may accordingly not be valid to assign the edge to the same value of the absorption coefficient, as is done in Fig. 2 of reference 21, after the bands have crossed.

IV. SCATTERING MECHANISMS

Of the scattering mechanisms that determine the transport properties of *n*-type GaAs, the most important above room temperature is the polar interaction. This mechanism has been shown by the author⁹ to be dominant in pure InSb, InP, and InAs at room temperature and above, but below temperatures in the narrow gap compounds where electron-hole scattering is important.

The parameters appearing in the electron-phonon interaction Hamiltonian in this case are all directly determinable from other experiments, so that one can calculate the transport properties without resort to adjustable constants. The calculations themselves are complicated by the fact that the relaxation-time approximation is not valid, so that it becomes necessary to invoke variational procedures. On the other hand, the 3-5 compounds, unlike the alkali halides or silver salts, are weakly polar. Thus, weak coupling theory suffices, and the conventional construction of the collision term of the Boltzmann equation is valid. When reasonably large concentrations of electrons are present in the semiconductor the polar interaction is screened.³⁵

The character of all the impurity scattering mechanisms in the 3-5 compounds is not yet fully understood.³⁶ However, in the samples having the highest mobility the principal scattering mechanism in this category over the temperature range of interest here appears to be charged impurity scattering as given by the familiar Brooks-Herring formula.²⁴ In the form used here, it has been adapted to apply to situations where Fermi statistics are relevant.⁹

³⁵ H. Ehrenreich, *J. Phys. Chem. Solids* **8**, 130 (1959).

³⁶ L. R. Weisberg and J. Blanc, *Bull. Am. Phys. Soc.* **5**, 62 (1960).

The effect of electron-electron scattering on this mechanism is known to be important³⁷ because Rutherford scattering is strongly dependent on the electron velocity. However, because present calculations emphasize regions of temperature and impurity concentration where lattice scattering predominates and because there are still experimental uncertainties concerning the character of the impurities in heavily doped low-mobility samples, it was not thought worthwhile to enter on the considerable complications to be encountered when this mechanism is included. In principle, however, such a calculation is feasible with the help of the variational technique given recently by McLean and Paige.³⁸

Deformation potential scattering, which is of great importance in germanium and silicon, is generally less significant in polar crystals. This is because (1) the coupling constant associated with the polar interaction is generally larger, (2) the importance of polar scattering is emphasized when the effective mass is small since $\mu(\text{def. pot.}) \sim m_1^{-2.5}$ whereas $\mu(\text{polar}) \sim m_1^{-1.5}$, and (3) piezoelectric scattering contributes in crystals lacking inversion symmetry. However, because the temperature dependence of the mobility resulting from deformation potential scattering is $T^{-1.5}$ as compared to the high-temperature variation of $T^{-0.5}$ of the mobility due to polar scattering, this mechanism may begin to play a role in polar materials with reasonably large band gaps at higher temperatures. This appears to be the case in GaAs. Further because point (2) loses its relevancy in the case of multivalley conduction bands, we shall see that in the subsidiary minima deformation potential scattering may be comparable to polar scattering.

The importance piezoelectric scattering in 3-5 compounds³⁹ has never been fully determined, because of the absence of measurements of the piezoelectric constants for these compounds. There is little reason to believe that this mechanism need be considered here above about 100°K. However, in the admittedly unlikely event that the constant should turn out to be as large in GaAs as that recently found for ZnO,⁴⁰ it should have to be taken quite seriously.

Nonpolar optical mode scattering, such as that found in germanium,⁴¹ vanishes for bands having *s* symmetry such as the [000] minimum of GaAs and does not need to be considered here.

V. TRANSPORT PROPERTIES

The drift mobility resulting from polar and charged impurity scattering may be written in the form

$$\begin{aligned} \mu(\text{cm}^2/\text{volt-sec}) &= 0.176(T/300)^{\frac{3}{2}}(e/e^*)^2(m/m_1)^{\frac{3}{2}}(10^{22}M) \\ &\quad \times (10^{23}v_a)(10^{-13}\omega_l)(e^2 - 1)F_{\frac{3}{2}}^{-1}(z)G_1(z, \vartheta), \quad (15) \end{aligned}$$

³⁷ L. Spitzer and R. Härm, *Phys. Rev.* **89**, 977 (1953).

³⁸ S. T. P. McLean and E. G. S. Paige, *J. Phys. Chem. Solids* (to be published).

³⁹ W. A. Harrison, *Phys. Rev.* **100**, 903 (1956).

⁴⁰ A. R. Hutson, *Phys. Rev. Letters* **4**, 505 (1960).

⁴¹ H. Ehrenreich and A. W. Overhauser, *Phys. Rev.* **104**, 331 and 649 (1956).

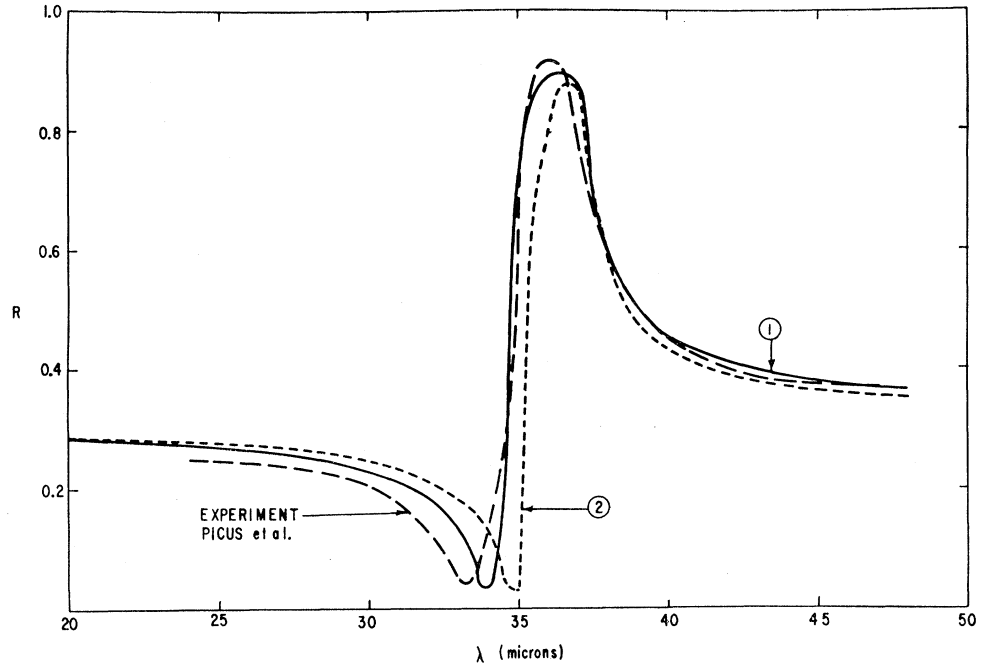


FIG. 6. Reflectivity vs wavelength. Curve (1) calculated from Eqs. (18) and (19) using $\hbar\omega_l = 0.036$ ev, $\epsilon_0 = 13.5$, $\epsilon_\infty = 11.6$, $\alpha = 0.01$. Curve (2) calculated from parameters deduced by Picus *et al.* and $\alpha = 0.01$.

where M is the reduced mass of the two ions in the unit cell, v_a is the volume of the cell, ω_l is the longitudinal optical frequency, and $z = \hbar\omega_l/KT$. The quantity e^* is the effective ionic charge, whose physical significance is discussed in reference 9. It depends only on ϵ_0 and ϵ_∞ , the static and dynamic dielectric constants, ω_l , the longitudinal optical frequency, v_a , and M , all of which can be determined experimentally. It may be written in the following convenient form:

$$(e^*/e)^2 = 0.0345(10^{22}M)(10^{-13}\omega_l)^2 \times (10^{23}v_a)(\epsilon_\infty^{-1} - \epsilon_0^{-1}). \quad (16)$$

The function G_1 containing the effects of the combined scattering mechanisms, is calculated with the help of the variational principle. Numerical results applicable when Boltzmann statistics, parabolic bands, and screening effects are taken into account are given in reference 35.⁴² In the present treatment, we shall calculate G_1 for properly combined polar and charged impurity scattering, taking into account both Fermi statistics and screening effects. The conduction band at [000] will be assumed to be of simple parabolic form, and scattering between the [000] and the subsidiary band edge will be neglected. The results necessary to calculate G_1 are given in the Appendix.

In choosing numerical values for the parameters to be substituted into Eq. (15) in connection with the present calculations, we find the only difficulty to be associated with the determination of e^* . The constants entering e^* can be obtained from an analysis of the optical re-

flectivity data of Picus *et al.*⁴³ in the vicinity of the reststrahlen peak, using the semiempirical expression for the frequency-dependent dielectric constant⁴⁴

$$\epsilon(\omega) = \epsilon_\infty + (\epsilon_0 - \epsilon_\infty) \frac{1 - (\omega/\omega_l)^2 - i(\omega/\omega_l)\alpha}{(n + ik)^2}, \quad (18)$$

and the familiar expression for the reflectivity

$$R = \frac{[(n-1)^2 + k^2]}{[(n+1)^2 + k^2]}. \quad (19)$$

We have attempted to obtain a detailed fit of the experimental data of reference 43. The results are shown by curve (1) of Fig. 6 in comparison to the data. The parameters used to obtain this curve are $\hbar\omega_l = 0.036$ ev, $\epsilon_0 = 13.5$, $\epsilon_\infty = 11.6$, and $\alpha = 0.01$. The value of $\hbar\omega_l = 0.036$ ev is confirmed by rather accurate measurements on GaAs tunnel diodes.⁴⁵ The effective ionic charge computed from this fit is $e^*/e = 0.186$. Curve (2) which agrees less well, is plotted using the parameters quoted by Picus *et al.*, but with the same value of α as in curve (1). With these values one arrives at the result $e^*/e = 0.17$. Since $\mu \sim (e/e^*)^2$ this difference accounts for a 20% change in the calculated mobility, which is perhaps typical of the error to be expected from this source.

The results of the calculation are shown in Fig. 7 as a function of temperature together with experimental results of Whelan and Wheatley²³ and Miller and Reid.⁴⁶ These samples have quoted impurity concen-

⁴³ G. Picus, E. Burstein, B. W. Hennis, and M. Hass, *J. Phys. Chem. Solids* 8, 282 (1959).

⁴⁴ M. Born and K. Huang, *Dynamical Theory of Crystal Lattices* (Oxford University Press, New York, 1954), p. 46.

⁴⁵ R. N. Hall, J. H. Racette, and H. Ehrenreich, *Phys. Rev. Letters* 4, 456 (1960).

⁴⁶ S. E. Miller and F. J. Reid, Report to Compound Semiconductor Research Group, Battelle Memorial Institute, 1959 (unpublished).

⁴² The notation in reference 35 differs from that used here. The symbols ω , z , and ξ of reference 35 are here and in references 9 and 10, ω_l , ϑ , and z , respectively.

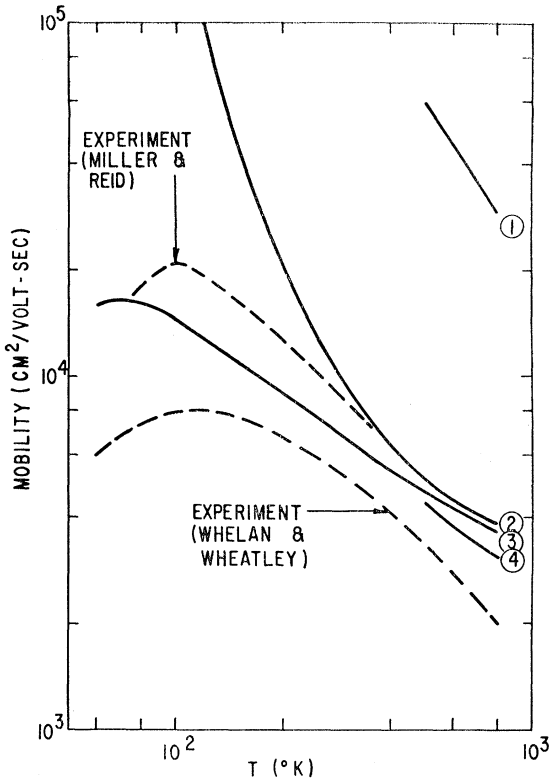


FIG. 7. Electron mobility vs temperature. Calculated curves: (1) deformation potential scattering; (2) screened polar scattering; (3) combined polar and charged impurity scattering ($n_I = 2.2 \times 10^{16} \text{ cm}^{-3}$); (4) combined polar, charged impurity, and deformation potential scattering, including effects of nonparabolic conduction band.

trations of $2.2 \times 10^{16} \text{ cm}^{-3}$ and $3.7 \times 10^{15} \text{ cm}^{-3}$, respectively. Our calculations assume the impurity concentration of the former sample. It should be noted that the experimental data represent Hall mobilities, whereas Eq. (15) represents a drift mobility. We may neglect this distinction here to good approximation because of the large value of the mobility ratio b and the factor in the Hall coefficient depending on the relaxation time is closely unity for polar scattering. Curve (1) represents the contribution of deformation potential scattering calculated for a simple s band from the Bardeen-Shockley theory.⁴⁷ The deformation potential constant E_1 may be estimated fairly well from the measured elastic constants⁴⁸ and the pressure experiments. Using the relationship $E_1 \approx -\kappa^{-1}(\partial E_{000}/\partial P)_T$, where κ is the compressibility, we find $E_1 = -7.0 \text{ eV}$, which is close to the value obtained for InSb. The longitudinal sound velocity was calculated from the elastic constants and appropriately averaged over the principal cubic directions. Curve (2) shows the mobility as a function of temperature for polar scattering alone, (including screening effects) and curve (3) the results obtained

⁴⁷ J. Bardeen and W. Shockley, *Phys. Rev.* **80**, 72 (1950).

⁴⁸ T. B. Bateman, H. J. McSkimin, and J. M. Whelan, *J. Appl. Phys.* **30**, 544 (1959).

when polar and charged impurity scattering are properly combined as indicated in the Appendix. In the former case the mobility is seen to have the exponential dependence at lower temperatures which is typical of polar scattering. At temperatures $T > \hbar\omega_1/K$ the curve begins to approach its asymptotic $T^{-3/2}$ dependence. Charged impurity scattering is seen to be important at low temperatures, causing the mobility to have a maximum at about 75°K. Curve (4) includes the effects of deformation potential scattering and the nonparabolicity of the conduction band which may be expected to become more important as increasingly energetic portions of the band become occupied. These are seen to lower the mobility only slightly. A similar effect would be produced if the mobility ratio b were smaller, and it was therefore necessary to consider the Hall mobility explicitly. For $b \approx 10$ the calculated Hall mobility would be lowered approximately in the way required by the experimental observations. Under the present assumptions concerning b , conduction in the subsidiary minima makes no contribution to the mobilities shown in Fig. 7.

In comparing our results with experiment, it should be remembered that an error of 20–30% in the calculation is to be expected, arising principally from (1) the uncertainty in e^* , (2) the use of $m_1 = 0.072m$ and the subsequent neglect of nonparabolic effects, and (3) the approximate nature of the variational calculation, which in the present case should certainly amount to less than 10% in the total error. Thus the agreement between theory and experiment must be considered to be satisfactory. It is nevertheless clear that at higher temperatures, where impurity scattering is unimportant, the agreement with a reasonable extrapolation of the experimental curve of Miller and Reid is best. This sample has exhibited the highest mobility (about 8500 $\text{cm}^2/\text{volt-sec}$ at room temperature) yet observed in n -type GaAs. The sample of Whelan and Wheatley is somewhat less pure. If the difference in mobility of the two samples were due solely to different amounts of ionized impurity scattering, the mobility above room temperature in the two samples should be the same. Also, at lower temperatures where polar scattering is no longer dominant our results should correspond exactly to the curve given by Whelan and Wheatley. The fact that neither of these conditions is satisfied may be indicative of the presence of another impurity scattering mechanism in the lower-mobility sample that varies very slowly with temperature. This qualitatively is in accord with the suggestions made by Weisberg and Blanc.³⁶

The role of impurity scattering is elucidated somewhat more completely in Fig. 8 which shows the mobility at room temperature as a function of ionized impurity concentration. The experimental points are the results of Reid and Willardson,⁴⁹ and Weisberg *et al.*,⁵⁰ and

⁴⁹ F. J. Reid and R. K. Willardson, *J. Elect. and Control* **5**, 54 (1958).

⁵⁰ L. R. Weisberg, J. R. Woolston, and M. Glicksman, *J. Appl. Phys.* **29**, 1514 (1958).

represent the highest value of the mobility that has been observed for a group of samples all having the same carrier concentrations as deduced from Hall measurements. The calculated curve for properly combined polar and charged impurity scattering agrees fairly well with the three experimental points corresponding to the samples having the lowest impurity concentration. Above concentrations of 10^{18} cm^{-3} the calculated curve is approximately 40% higher than the experimental points. This discrepancy can be accounted for by electron-electron scattering, which we have not considered here. It should be emphasized, however, that there is no reason to expect validity of the Brooks-Herring formula for such large impurity concentrations.

The limiting value of the mobility for a perfectly pure sample is $9300 \text{ cm}^2/\text{volt-sec}$ at room temperature due to polar scattering alone. This is somewhat lower than the result obtained by Weisberg *et al.*⁵⁰ on the basis of an extrapolation of a curve similar to Fig. 8.

The thermoelectric power Q is given by the expression

$$Q = (K/e)(A - z). \quad (17)$$

The quantity A here is the so-called transport term which is but weakly dependent on the scattering mechanism. In references 9 and 10 we calculated A variationally. Here we shall use the results of Delves⁵¹ which apply to purely polar scattering, parabolic bands, and Fermi statistics. Since our treatment of the thermoelectric power will neglect impurity scattering, we shall confine our comparison with experiments to the region above room temperature. Figure 9 shows the calculated results compared to data on two specimens obtained by Edmond *et al.*²⁰ the upper curve corresponding to a carrier concentration $8.5 \times 10^{16} \text{ cm}^{-3}$ and the lower to $9.0 \times 10^{17} \text{ cm}^{-3}$. Unfortunately, no conductivity data are

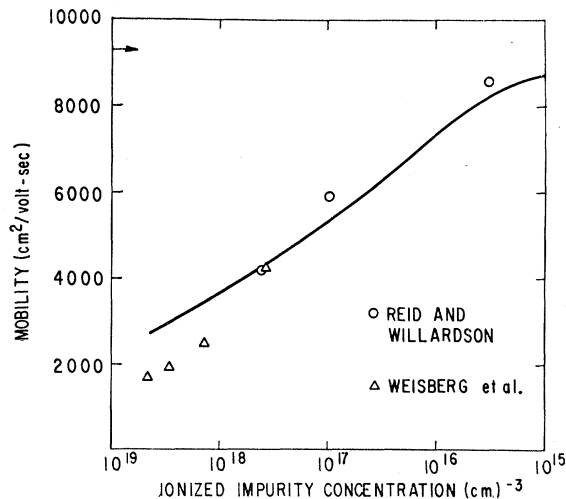


FIG. 8. Calculated electron mobility vs ionized impurity concentration at 300°K for properly combined polar and charged impurity scattering. Arrow indicates limiting mobility for polar scattering in pure sample.

⁵¹ R. T. Delves, Proc. Phys. Soc. (London) **73**, 572 (1959).

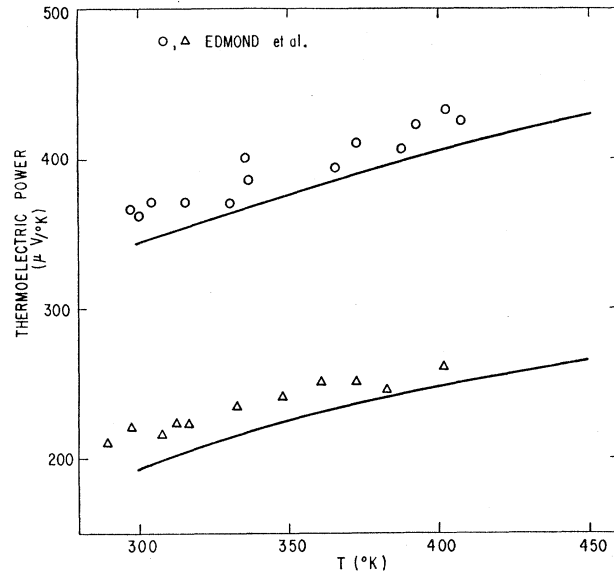


FIG. 9. Thermoelectric power vs temperature. Experimental points: \circ $n = 8.5 \times 10^{16} \text{ cm}^{-3}$; \triangle $9.0 \times 10^{17} \text{ cm}^{-3}$; theoretical curve for polar scattering and Fermi statistics.

given, so that it is impossible to be certain that the samples are sufficiently pure that polar scattering is indeed dominant in the temperature range between 400 and 500°K . The agreement between theory and experiment is within 10% and probably reflects more the accuracy of the calculation of the Fermi level than the use of the correct scattering mechanism. The fact that the theoretical curves are below the experimental points in both cases may indicate the presence of some impurity scattering since A is a bit larger for this mechanism than for polar scattering.

We shall conclude this section with some qualitative remarks concerning the mobility in the subsidiary minima and the role of intervalley scattering. Both the pressure experiments and the Hall data indicate that the mobility in band 2 may be fifty times, or more, smaller than that in band 1. The pressure experiments were seen to be more sensitive to b , since any saturation of the increase of resistivity with pressure would be associated with the value of b according to the present considerations. Unfortunately, the samples used by Howard and Paul were apparently characterized by a rather low mobility ($\sim 1800 \text{ cm}^2/\text{volt-sec}$ at 300°K for one of the samples), so that polar scattering probably was not predominant at room temperature. However, since the two samples did not differ appreciably in their behavior at high pressures, it is probable that the large mobility ratio deduced from the data results not so much from any peculiar scattering mechanisms but rather from the fact that the anisotropy mass ratio $K = m_{11}/m_1$ of the ellipsoidal valleys is fairly small and hence the density of states for scattering in band 2 is large. This is further borne out by the fact that m_p was estimated to be larger than that in Si.

The consistency of the large density of states mass on the one hand with the low mobility in band 2 on the other may be examined by means of a rough calculation of the mobility. We shall assume that both polar and deformation potential scattering are operative and take the ellipticity of the valleys into account by replacing the mass dependence m^{-n} in the expressions for the mobility for the two scattering mechanisms ($n=\frac{3}{2}$ for polar and $n=\frac{5}{2}$ for deformation potential scattering) by

$$m^{-n} \rightarrow m_I^{-1} \bar{m}^{-(n-1)}. \quad (18)$$

Here $\bar{m} = m_p / \nu^{\frac{2}{3}} = (m_{11} m_{12}^2)^{\frac{1}{3}}$ is the geometric mean of the masses in one ellipsoid, ν corresponds to the number of equivalent valleys, and $m_I^{-1} = \frac{1}{3}(m_{11}^{-1} + 2m_{12}^{-1})$ is the conductivity mass. The use of Eq. (18) in conjunction with Eq. (15) to calculate the contribution of polar scattering in ellipsoidal valleys, keeping $G^{(0)}$ as before, has been shown to be good to about 10% by comparison with detailed variational calculations by the author which treat the problem correctly.⁵² The use of Eq. (18) in conjunction with deformation potential scattering is discussed by Brooks.²⁴ We shall assume $m_{11} = 0.98m$ as in Si, and adjust K to yield $m_p = 1.2(+0.5, -0.3)m$ deduced earlier. Calculating the mobilities and combining according to the simple relationship $\mu^{-1} = \mu_{DP}^{-1} + \mu_{polar}^{-1}$ we find for $m_p = 1.2m$ that $K = 4.5$ and $b = 18$, whereas for $m_p = 1.7m$ that $K = 2.6$ and $b = 40$. Polar and deformation potential scattering are found to be about equally important: $\mu_{DP} \approx \mu_{polar} \approx 1000$ cm²/volt-sec in the first case, and about 450 cm²/volt-sec in the second case.

It is seen that the large mobility ratio demanded by the pressure experiments is not inconsistent with the values of the density of states mass, although the values of b obtained from the preceding estimate are a bit on the low side. Since, however, we have assumed $b = b^*$, a small temperature variation of ΔE could easily lead to even smaller K .

The transport theory given in this paper has consistently neglected interband and intervalley scattering. This may be justified for polar scattering on the grounds that the probability for scattering is weighted in the forward direction. Thus the ratio of the squares of the matrix elements for intra- to inter-band scattering is of order $(K/k)^2$ where $k \sim (2m_1 KT)^{\frac{1}{2}}/\hbar$ is a typical electron wave vector in the distribution and K is a reciprocal lattice vector. For GaAs at room temperature $(K/k)^2 \approx 1600$. This factor describes the relative importance of intervalley scattering among the subsidiary minima due to the polar interaction alone and shows it to be negligible. In discussing interband scattering from band 1 to 2 at elevated temperatures or pressures, we must divide this factor by $(m_p/m_1)^{\frac{2}{3}} \approx 70$ due to the larger density of states in band 2. This effect is also insignificant. However, the nonpolar interactions such as deformation potential scattering may contribute significantly to intervalley scattering.

⁵² H. Ehrenreich (unpublished).

VI. COMMENTS

The conclusions concerning the effective mass and transport properties in the [000] conduction band discussed in this paper are believed to be fairly firmly established. By contrast, the evidence concerning the symmetry and masses of the subsidiary conduction band minima is much more circumstantial. There are several factors which make it likely that these minima are located along [100] directions: (1) Extrapolation of the band gaps observed in Ga(As,P) alloys indicates the [100] minima to be located energetically where the Hall and pressure experiments place the subsidiary edge; (2) The shift of the subsidiary edge with pressure is probably negative; (3) The density of states effective mass is large, and the mass anisotropy ratio is reasonably small as in silicon. More direct experimental evidence concerning band 2 will be difficult to obtain if the mobility ratio b in fact is as large in pure samples as indicated by the pressure experiments discussed here. Except for the Hall effect, most transport properties involving band 2 are weighted by the factor

$$(b_p^*/b) \exp[-\Delta E(0)/KT], \quad (19)$$

which, even though $b_p^* \approx b$, is very small (~ 0.02 at 1000°K) in the case of GaAs because ΔE is rather large. The reason why the Hall effect reflects the presence of the subsidiary edge is evident from Eq. (6): the factor b which appreciably reduces the magnitude of (19) is not present. Thus the possibility of elasto-resistance or magnetoresistance measurements at high temperatures, which might ordinarily provide direct evidence concerning the symmetry of the minima, appears to be rather remote unless the experiments are performed at sufficiently high pressure that all the conduction takes place in the subsidiary minima.

ACKNOWLEDGMENTS

This work was begun in collaboration with P. V. Gray and was continued with the very capable help of Doris J. Olechna. In addition, for invaluable discussions of data, and for making results available, I should like to express my thanks to L. W. Aukerman, A. C. Beer, R. Braunstein, H. G. Drickamer, W. Howard, W. Paul, G. Picus, A. Sagar, W. Spitzer, and L. R. Weisberg. I am indebted to the members of the Compound Semiconductor Research group at Battelle Memorial Institute for permission to quote data.

APPENDIX

We present the results necessary for the evaluation of the function G_1 , which leads immediately to the mobility via Eq. (15) in Sec. IV. This is a special case of the equation derived by the author in reference 10.⁵³ The results assume (1) parabolic bands having s symmetry,

⁵³ Numbered equations from this reference used in this Appendix will be prefaced with I.

(2) Fermi statistics, (3) combined charged impurity and polar scattering, and (4) that screening effects in connection with the polar interaction are taken into account. The variational trial function is taken to have the form (I, 54.2). To the approximation used in the present calculations we obtain

$$G_1 = \frac{\langle 0|x^3\rangle^2}{\langle 0|\mathcal{L}|0\rangle} + \left\{ \frac{\left| \begin{matrix} \langle 0|\mathcal{L}|0\rangle & \langle 0|x^3\rangle \\ \langle 1|\mathcal{L}|0\rangle & \langle 1|x^3\rangle \end{matrix} \right|^2}{\left| \begin{matrix} \langle 0|\mathcal{L}|0\rangle & \langle 0|\mathcal{L}|1\rangle \\ \langle 1|\mathcal{L}|0\rangle & \langle 1|\mathcal{L}|1\rangle \end{matrix} \right|} \langle 0|\mathcal{L}|0\rangle \right. \\ \left. + \frac{\left\{ \begin{matrix} \langle 0|\mathcal{L}|0\rangle & \langle 0|\mathcal{L}|1\rangle & \langle 0|x^3\rangle \\ \langle 1|\mathcal{L}|0\rangle & \langle 1|\mathcal{L}|1\rangle & \langle 1|x^3\rangle \\ \langle 2|\mathcal{L}|0\rangle & \langle 2|\mathcal{L}|1\rangle & \langle 2|x^3\rangle \end{matrix} \right\}^2}{\left| \begin{matrix} \langle 0|\mathcal{L}|0\rangle & \langle 0|\mathcal{L}|1\rangle & \langle 0|\mathcal{L}|2\rangle \\ \langle 1|\mathcal{L}|0\rangle & \langle 1|\mathcal{L}|1\rangle & \langle 1|\mathcal{L}|2\rangle \\ \langle 2|\mathcal{L}|0\rangle & \langle 2|\mathcal{L}|1\rangle & \langle 2|\mathcal{L}|2\rangle \end{matrix} \right|} \left| \begin{matrix} \langle 0|\mathcal{L}|0\rangle & \langle 0|\mathcal{L}|1\rangle \\ \langle 1|\mathcal{L}|0\rangle & \langle 1|\mathcal{L}|1\rangle \end{matrix} \right|} \right. \quad (A1)$$

Here

$$\langle i|\mathcal{L}|j\rangle = \langle i|\mathcal{L}_A|j\rangle + \langle i|\mathcal{L}_B|j\rangle, \quad (A2)$$

\mathcal{L}_A and \mathcal{L}_B referring to the collision terms for polar and charged impurity scattering, respectively, and

$$\langle i|\mathcal{L}_A|j\rangle = \int_0^\infty dy [e^{y-z} + e^{-y}]^{-1} [1 + e^{-(y-z)}]^{-1} [S_+' y^{-1} (y^{i+i+1} + y_+^{i+i+1}) - R_+' (y_+^i y^i + y_+^j y^j)], \quad (A3)$$

$$\langle i|\mathcal{L}_B|j\rangle = (e^\vartheta - 1) \hbar M v_a \omega_i m (e/e^*)^2 / 4m_1 \epsilon^2 K T \int_0^\infty dy f_0 (1 - f_0) y^i y^j [\ln(1 + 8y/\vartheta P^2) - (1 + \vartheta P^2/8y)^{-1}], \quad (A4)$$

where

$$R_+' = \frac{1}{4} (y_+ + y + \vartheta P^2) \ln \left\{ \frac{[(y_+^{\frac{1}{2}} + y^{\frac{1}{2}})^2 + \frac{1}{2} \vartheta P^2]}{[(y_+^{\frac{1}{2}} - y^{\frac{1}{2}})^2 + \frac{1}{2} \vartheta P^2]} \right\} \\ - (y y_+)^{\frac{1}{2}} [\vartheta^2 + \frac{1}{2} \vartheta P^2 (3y_+ + 3y + \vartheta P^2)] / [\vartheta^2 + \vartheta P^2 (y_+ + y + \frac{1}{4} \vartheta P^2)], \quad (A5)$$

$$y^{-1} S_+' = - (y y_+)^{\frac{1}{2}} \vartheta P^2 [\vartheta^2 + \vartheta P^2 (y_+ + y + \frac{1}{4} \vartheta P^2)]^{-1} + \frac{1}{2} \ln \left\{ \frac{[(y_+^{\frac{1}{2}} + y^{\frac{1}{2}})^2 + \frac{1}{2} \vartheta P^2]}{[(y_+^{\frac{1}{2}} - y^{\frac{1}{2}})^2 + \frac{1}{2} \vartheta P^2]} \right\},$$

and $y = E/KT$, $z = \zeta/KT$, $\vartheta = \hbar\omega_i/KT$, $y_+ = y + \vartheta$, $\vartheta P^2 = (4\pi n e^2 / \epsilon m^*) (\hbar/KT)^2 (d/dz) \ln F_{\frac{1}{2}}(z)$, $f_0 = [e^{y-z} + 1]^{-1}$; ζ is the Fermi energy, and $F_{\frac{1}{2}}(z)$ is a Fermi-Dirac integral.

Equations (A1), (A2), (A3), and (A5) are obtained in straightforward fashion from Eqs. (I, 47), (I, 23), (I, 52), and (I, 20)⁵⁴ respectively. The primes on R and S indi-

cate that these differ from the corresponding quantities in I by the factors $\beta^* = KT/E_G^*$. An inherent feature of the variational principle used here is that successive terms in the preceding series for G_1 are all positive. In the present calculations, the last term provides a correction of at most 10% at low temperatures, and becomes less important with increasing temperatures.

⁵⁴ multiplied by a factor x , which was omitted due to a typographical error.

⁵⁴ The integrand of the equation for R_\pm in (I, 20) should be